

Original Article

SPECTRO-ANALYTICAL, COMPUTATIONAL AND BIOLOGICAL STUDIES ON 4-PYRIDINE CARBOXALDEHYDE-3-HYDROXY-5-(HYDROXY METHYL)-2-METHYL HYDRAZONE HYDROCHLORIDE AND ITS CU (II) COMPLEXCA

<sup>a</sup>K. ESHWARI, <sup>b</sup>P. MAMTHA, <sup>c</sup>M. RAVI, <sup>d</sup>B. APARNA, <sup>a</sup>P. HARILATHA REDDY, <sup>c\*</sup>C. H. SARALA DEVI

<sup>a</sup>Department of chemistry, S.N.Vanitha Mahavidyalaya, Hyderabad 500001, TS, India, <sup>b</sup>Department of chemistry, University college for Women, Koti, Hyderabad -500095, TS, India, <sup>c\*</sup>Department of chemistry, University College of Science, Osmania University, Hyderabad 500007, TS, India, <sup>d</sup>Department of chemistry, Nizam college, Hyderabad 500001, TS, India.  
Email: dr\_saraladevich@yahoo.com

Received: 20 Jun 2014 Revised and Accepted: 22 Jul 2014

ABSTRACT

**Objective:** The title compound 4-pyridine carboxaldehyde 3-hydroxy-5-(hydroxy methyl)-2-methyl hydrazone (PCHHMMH) hydrochloride an analogue of Pyridoxal isonicotinoyl hydrazone PIH, is an iron chelator. The PCHHMMH has potential donor sites suitable for metal ion binding, the study on structural aspects of the compound and its copper complex are explored. With a view to understand biological importance of title compounds, antimicrobial and cytotoxic studies were planned.

**Methods:** In the present study the spectroanalytical techniques employed were pH-metry, spectrophotometry, IR, <sup>1</sup>H & <sup>13</sup>C-NMR, UV-Vis, ESR, Magnetic measurements, TGA and SEM. The computational method employed is HyperChem 7.5 software. The antimicrobial studies were carried out by agar disc diffusion method for antibacterial studies against Gram positive and Gram negative bacteria. The cytotoxic potential was measured by Sulforhodamine B (SRB) method against selected tumor cells.

**Results:** The equilibrium studies by employing pH-metric method inferred the dissociation of two protons in it. Further titration in presence of Cu (II) ion, it is confirmed the release of two protons from title compound and formation of corresponding complex. The orientations of frontier orbitals for molecular and ionized forms of compound were computed to understand the electronic properties. The Cu (II) PCHHMMH complex was characterized by spectroanalytical methods and screened for, antimicrobial and cytotoxic activities.

**Conclusion:** As the structural features are important to understand the chemical behavior of metal complexes, in the present study copper complex was synthesized and characterized by employing various spectro-analytical tools viz; IR, <sup>1</sup>H & <sup>13</sup>C-NMR, UV-Vis, ESR, Magnetic measurements, TGA and SEM. Further the antimicrobial and cytotoxic activities were evaluated and correlated with computed QSAR data.

**Keywords:** 4-pyridine carboxaldehyde-3-hydroxy-5-(hydroxy methyl)-2-methyl hydrazone (PCHHMMH) hydrochloride, DEPT, HyperChem 7.5, Cu (II) PCHHMMH complex and ESR studies.

INTRODUCTION

Iron chelating agents are essential for treating iron overload which is a consequence of long-term transfusion therapy in the disease  $\beta$ -thalassemia and are potentially useful for therapy in non-haeme iron[1,2,3] overload conditions. According to previous studies the tridentate chelator Pyridoxal isonicotinoyl hydrazone (PIH) has high iron chelation efficacy in vitro and vivo with high selectivity and affinity for iron [4]. Most biological studies on PIH analogues inferred their effective binding with metal ions [5]. Hence, in the present investigation, we have planned for spectro-analytical properties of pyridoxal hydrazone viz; 4-pyridine carboxaldehyde-3-hydroxy-5-(hydroxy methyl)-2-methyl hydrazone (PCHHMMH) hydrochloride to explore its metal binding properties. Further its Cu (II) complex is synthesized to understand its activity in various biological applications including cytotoxicity.

MATERIALS AND METHODS

All the chemicals used are AR Grade. Pyridoxal Hydrochloride is procured from Sigma Aldrich and Hydrazine Hydrate from MERCK.

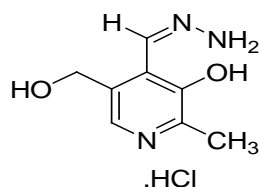


Fig. 1: Pyridine carboxaldehyde-3-hydroxy-5-(hydroxy methyl)-2-methyl hydrazone (PCHHMMH) hydrochloride

The 4-Pyridine carboxaldehyde-3-hydroxy-5-(hydroxymethyl)-2-methyl hydrazone (PCHHMMH) hydrochloride (Fig.1) was synthesized using known procedure [6]. The purity of compound was ascertained by recording LC-MS data on Shimadzu LCMS-2010A. The chromatogram was obtained by injecting 5 $\mu$ L of the sample dissolved in methanol into C18 column, using methanol: water mobile phase mixture 90:10, with a flow rate 0.2 mL/min and UV (254 nm) detector. The mass spectrum obtained by using Atmospheric Pressure Chemical Ionization in Negative Mode. The Cu (II) complex of title compound was synthesized by known procedure and its mass was recorded on VG AUTOSPEC. IR spectra (KBr) were recorded on a Perkin-Elmer 435 spectrophotometer. <sup>1</sup>H-NMR and <sup>13</sup>C-NMR spectra were recorded on Bruker WH (270 MHz) spectrometer. UV-Vis spectra were scanned on UV-3600 Shimadzu spectrophotometer.

The pH measurements were made using a digital ELICO electronic model LI 120 pH meter in conjunction with a combined glass and calomel electrode. The pH meter was calibrated at different pH values 7.0, 4.0 and 9.2 using the appropriate standard (BDH) buffers with necessary temperature corrections. Irving-Rossotti pH [7, 8, 9] titration technique was employed for the determination of dissociation constants in aqueous medium. The magnetic susceptibility of the copper complex was measured on a Faraday balance model 7550. The calibration constant was first determined by taking a measurement on standard substance Hg[Co(SCN)<sub>4</sub>]. The particle size and morphology of Cu (II) PCHHMMH complex were recorded on Ziess Scanning Electron Microscope. INCA EDX instrument was used to study the elemental analysis. Thermo gravimetric analysis (TGA) [10, 11, 12] and differential thermal analyses (DTA) of complex was carried out on Shimadzu TGA-50 H

in the Nitrogen atmosphere in the temperature range 0-1000 °C. The ESR spectrum was recorded on BRUKER-EMX using X-band radiation. The molecular modeling program HyperChem 7.5 was employed for computational studies.

## RESULTS AND DISCUSSION

### Spectro analytical studies of PCHMMH

In order to understand structural aspects of title compound, IR,  $^1\text{H-NMR}$ ,  $^{13}\text{C-NMR}$ , DEPT and UV-Vis, spectra were recorded. To elucidate the number of dissociable protons and to know the binding sites in the title compound, pH-Metric studies were carried out.

### Mass spectrum

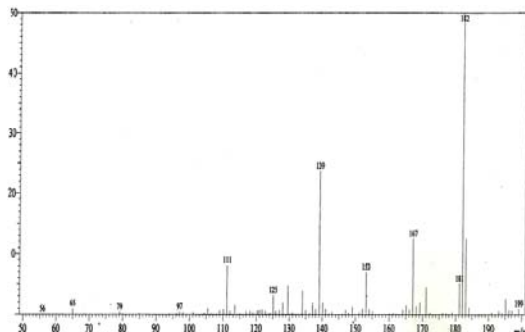


Fig. 2: Mass spectrum of PCHMMH

The mass spectrum of PCHMMH recorded a peak with maximum intensity (base peak) at  $m/z$  182 which corresponds to  $[\text{M}+\text{H}]^+$  and at  $m/z$  181 to  $[\text{M}]^+$  molecular ion peak. Other fragment peaks are observed at  $m/z$  167, 153, 139 and 125. The expected mass corresponding to hydrochloride form of PCHMMH is off the scale of mass spectrum.

### IR spectrum

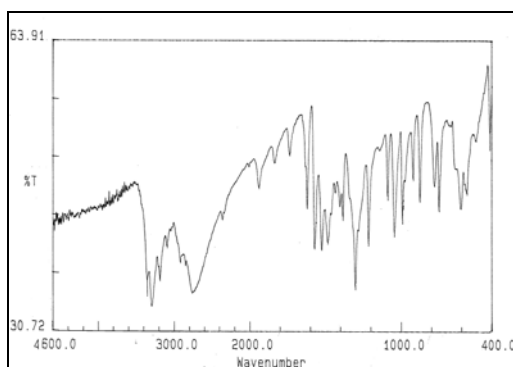


Fig. 3: IR Spectrum of PCHMMH

IR spectrum of compound displayed peaks at  $3354\text{ cm}^{-1}$  ( $\nu_{\text{O-H}}$ ),  $3292\text{ cm}^{-1}$  and  $3180\text{ cm}^{-1}$  ( $\nu_{\text{N-H}}$ ) symmetric and asymmetric stretching respectively. The peaks at  $3090\text{ cm}^{-1}$  ( $\nu_{\text{C-H (Arom)}}$ ),  $2914\text{ cm}^{-1}$  ( $\nu_{\text{C-H, CH}_3}$ ),  $1620\text{ cm}^{-1}$  ( $\nu_{\text{C=N}}$ ),  $1570\text{ cm}^{-1}$  ( $\nu_{\text{C=C}}$ ),  $1215\text{ cm}^{-1}$  ( $\text{CH}_3$  bending) and  $1089\text{ cm}^{-1}$  ( $\nu_{\text{C-O}}$ ) are also structurally supported vibrational IR active modes. The appearance of shoulder and broad nature of the band above  $3000\text{ cm}^{-1}$  indicates that extensive inter and intra molecular hydrogen bonding in the compound.

### $^1\text{H-NMR}$ & $\text{D}_2\text{O}$ Exchange

The  $^1\text{H-NMR}$  spectrum determined in  $\text{DMSO-d}_6$  showed peaks at  $12.89\text{ }\delta$  (s, Ar-OH),  $8.5\text{ }\delta$  (s,  $\text{NH}_2$ ),  $8.4\text{ }\delta$  (s,  $\text{CH=N}$ ),  $8.1\text{ }\delta$  (s, Ar-CH),  $5.6\text{ }\delta$  (s, alcoholic-OH),  $4.63$  (s,  $\text{CH}_2\text{-N=N}$ ),  $2.6$  (s,  $\text{CH}_2$ ),  $2.5$  (s,  $\text{CH}_3$ ) ppm. The  $\delta$  ( $\text{NH}_2$ ) and  $\delta$  (Ar-OH) peaks are confirmed by  $\text{D}_2\text{O}$  studies, which disappeared on deuteration (Fig.4a & Fig.4b).

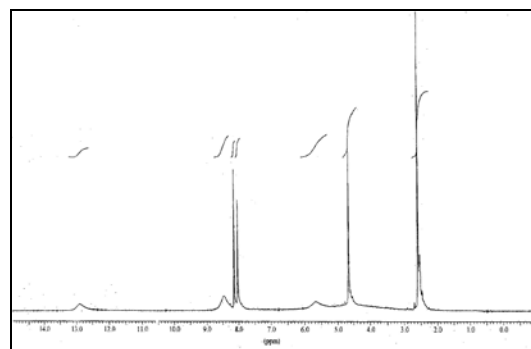


Fig. 4a:  $^1\text{H-NMR}$  spectrum in  $\text{DMSO-d}_6$

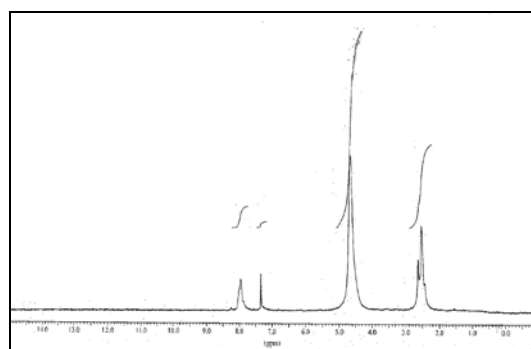


Fig. 4b  $\text{D}_2\text{O}$  exchange spectrum of PCHMMH

### $^{13}\text{C-NMR}$ & DEPT 135

The  $^{13}\text{C-NMR}$  recorded signals ( $\text{DMSO-d}_6$ ,  $\delta$ ) at 151, 140, 133, 132, 129, 128, 58 and 14.2 ppm correspond to aromatic, azomethine and aliphatic carbons respectively (Fig.5a).

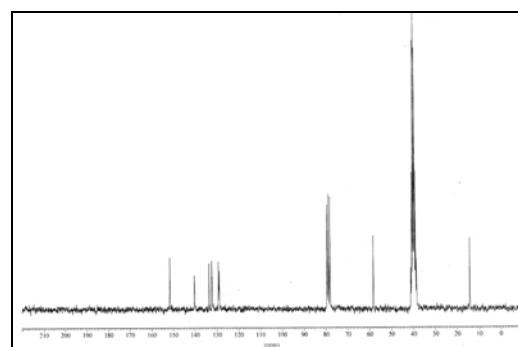


Fig. 5a:  $^{13}\text{C-NMR}$  spectrum of PCHMMH

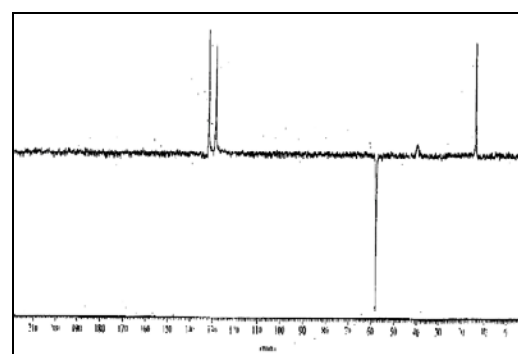


Fig. 5b: DEPT Spectrum of PCHMMH

The DEPT 135 spectrum (Fig.5b) indicated upward peaks of primary carbon at 14.2 ppm and tertiary carbons at 128, 133 ppm, and downward peak corresponding to secondary carbon at 58 ppm. The peaks observed in  $^{13}\text{C}$ -NMR (Fig.5a) at 151, 140, 132 and 129 are ascribable to quaternary carbon atoms.

The experimental data is compared with the theoretical data (Table 1, 2,3) obtained by the optimized structure of the molecule (Fig.6a) using Hyperchem 7.5 tools[13].

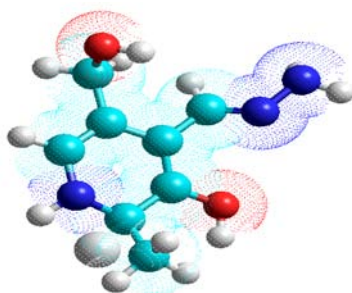


Fig. 6a: Geometry Optimized structure of PCHHMMH.HCl

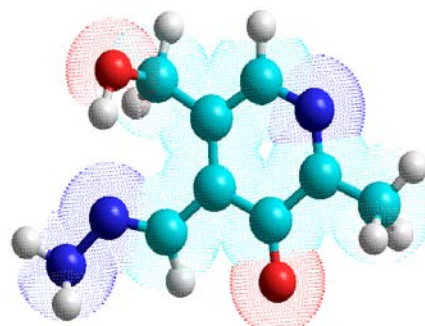


Fig. 6b: Geometry optimized structure for ionized form of PCHHMMH

#### IR spectral Analysis

The experimental IR spectral data and corresponding computed data (Table.1) generated through semi empirical single point PM3 method for optimized molecule (Fig.6a), are in good agreement.

Table 1: IR Spectral data of PCHHMMH

Compound	$\nu \text{ cm}^{-1}$						
PCHHMMH	$\text{CH}_2\text{OH, OH}$	NH	CH (Arom)	$\text{CH}_3$	C=N	C=C (ring)	C-O
Experimental	3400 -3300	3202, 3180	3090	2914	1620	1570	1089
Computed	3900-3800	3540,3408	3100	3165	1826	1594	1100

#### NMR Spectral Simulation

$^1\text{H}$ -NMR and  $^{13}\text{C}$ -NMR data were also computed and compared with the experimental data obtained (Table-2, 3). From the analysis of

data it is clear that there is deviation in chemical shift values with respect to protons attached to electronegative groups. Such deviations are attributable to hydrogen bonding interactions which would influence the experimental values.

Table 2:  $^1\text{H}$ -NMR  $\delta$ (ppm) Spectral Data of PCHHMMH

PCHHMMH	$\delta \text{ ppm}$						
	OH(ring)	NH	HC=N(azomethine)	CH(arom)	OH(benzylic)	$\text{CH}_2$	$\text{CH}_3$
Experimental	12.89	8.45	8.4	8.1	5.6	2.6	2.5
Computed	12.7	8.24	8.50	10.14	5.90	3.6	1.5

Table 3:  $^{13}\text{C}$ -NMR Spectral data

PCHHMMH	$\delta \text{ ppm}$				
	Aromatic carbons		HC=N	$\text{CH}_2$	$\text{CH}_3$
Experimental	151, 140,132,129,128		133	58	14.2
Computed	182,157,136,176,133		231	60	12

The  $^{13}\text{C}$  NMR chemical shifts, computed by Hyperchem tools showed comparable results with experimental values with more deviation corresponding to azomethine carbon.

#### pH- Metric studies

To understand the chelation properties of the title compound, an attempt is made to study its potential donor sites that bind with metal ions. The title compound is in hydrochloride form and hence ring nitrogen gets protonated in the solution. In the present investigation an attempt was made to determine dissociation constants by Irving-Rossotti pH-metric technique. The pH-metric titrations were carried out in aqueous medium at 303° K and 0.1 M ( $\text{KNO}_3$ ) ionic strength (Fig.7a).

The dissociation constant values were calculated using Irving-Rossotti titration curves. From the titration data obtained, dissociation constants have been calculated from the linear plots of  $\text{Log} \left( \frac{2-\bar{r}_A}{\bar{r}_A-1} \right)$ ,  $\text{Log} \left( \frac{1-\bar{r}_A}{\bar{r}_A} \right)$ , Vs pH (Fig.7b and 7c). The results indicated the presence of two dissociable protons corresponding to ring  $\text{NH}^+$  proton ( $pK_{a1}=4.7$ ) and phenolic OH group of PCHHMMH ( $pK_{a2}=10.58$ ).

The titration curves clearly indicated the release of dissociable protons more easily in presence of  $\text{Cu}^{2+}$  ions indicating formation of corresponding complex in solution.

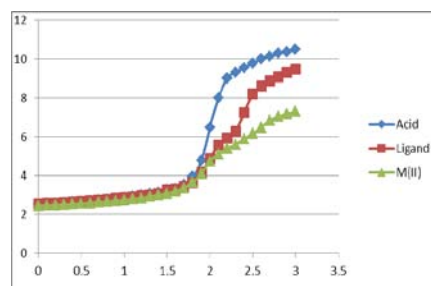


Fig. 7a: pH titration curves of PCHHMMH system in aqueous medium at 303 K and 0.1 M ionic strength

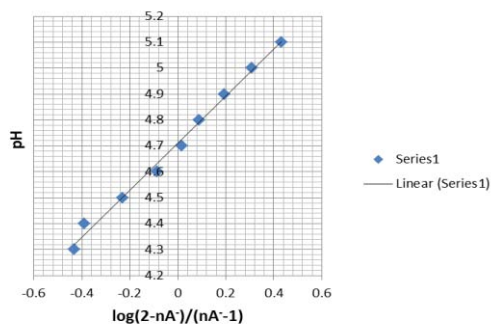


Fig. 7b: Plot of  $\text{Log} (2 - \alpha_A) / (\alpha_A - 1)$  Vs pH of PCHMMH in aqueous medium

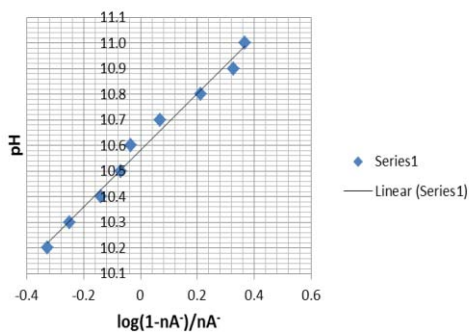


Fig. 7c: Plot of  $\text{Log} (1 - \alpha_A) / \alpha_A$  Vs pH of PCHMMH in aqueous medium

#### Spectrophotometric studies of PCHMMH and its interaction with Cu (II) metal ion.

An attempt was made to establish the metal to ligand ratio in the complex formed from PCHMMH and copper (II) ion, by adopting mole ratio method. A series of solutions are prepared [14], in which the molar concentration of metal ion is kept constant while that of the PCHMMH was varied. The pH of solutions was maintained constant by adding acetate buffer for 1:1 composition at 411 nm. A plot of the absorbance versus number of moles of the PCHMMH per mole of Cu (II) ion showed two straight lines of different slopes intersecting at a point corresponding to one mole of ligand (Fig.8) confirmed formation of 1:1 complex.

#### Computational Studies

In the present investigation the HyperChem 7.5 software was used for quantum mechanical calculations. After building molecule by HyperChem 7.5 tools [15-20], the geometry optimization was carried out using semi empirical single point PM3 method. The IR and NMR spectral data is generated with approximation for the title compound. Quantum chemical calculations have been widely used to

study donor and acceptor properties of molecules. The values of energy of the highest occupied molecular orbitals ( $E_{\text{HOMO}}$ ), the lowest unoccupied molecular orbitals ( $E_{\text{LUMO}}$ ) and the energy gap between  $E_{\text{HOMO}}$ - $E_{\text{LUMO}}$  were computed.

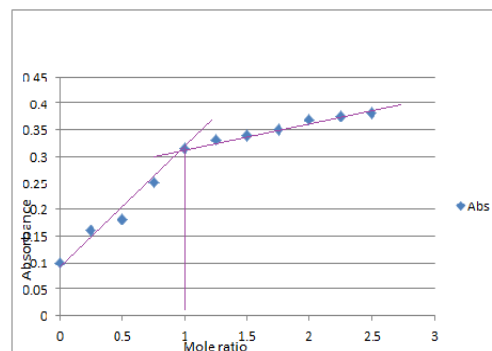


Fig. 8: Plot of absorbance versus mole ratio of ligand at 303 K in dilute acetic acid medium.

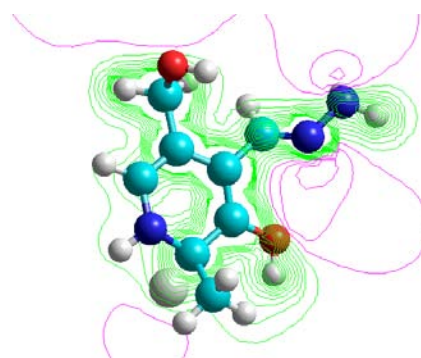


Fig. 9a: Contour Map of Electrostatic Potential of molecule

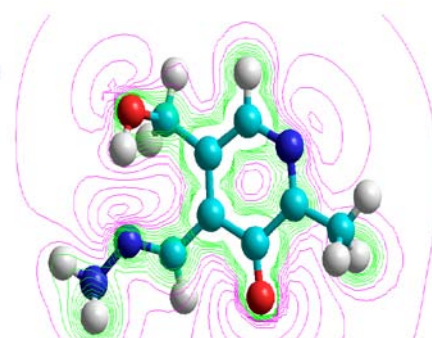


Fig. 9b: Electrostatic potential in ionized form

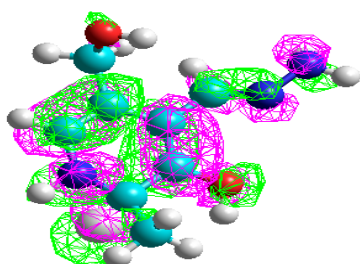


Fig.10a: Contour Map of Highest Occupied Molecular Orbital (HOMO)  
Eigen Value -8.26 eV

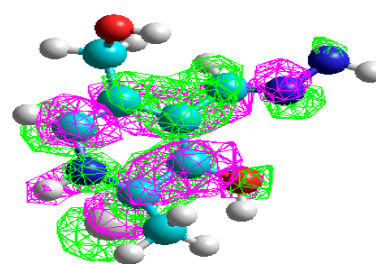
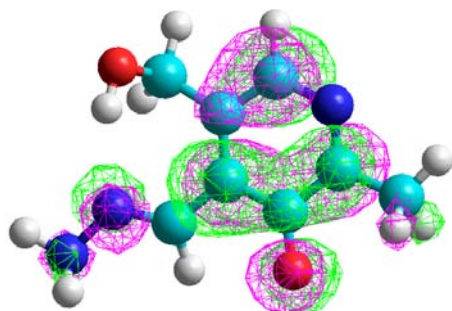


Fig.10b: Contour Map of Lowest Unoccupied Molecular Orbital (LUMO)  
Eigen Value -0.486 eV

The charge density sites and electrostatic potentials are localized more on phenolic oxygen and imine nitrogen (**Fig.9a, 9b**) in both the molecular and ionic forms. The orientation of highest occupied molecular orbitals (HOMO) and lowest unoccupied molecular orbitals (LUMO) are generated (**Fig.10a, 10b**) to understand the metal binding sites. The energy difference of 7.77eV between the HOMO (B.E: 8.26eV) and LUMO (B.E: 0.486eV) frontier orbitals in



**Fig. 11a: Highest Occupied Molecular Orbitals(HOMO)in Ionized Form**  
Eigen Value -3.71eV

The HOMO orientation in ionized form confirms that, the anti bonding orbitals oriented along oxygen of phenyl ring and imine nitrogen are more suitable for bonding.

#### Quantitative structure-activity relationship

Quantitative structure-activity relationship (QSAR) is a computational process that relates the chemical structure of

molecular form is more than the energy difference of 7.31 eV between HOMO (B.E 3.71 eV) and LUMO (B.E: -3.60 eV) orbitals in ionized form indicating relatively more labile property in latter.

The lower binding energy of HOMO frontier orbitals of ionic species incriminates greater binding ability in ionized form rather than in molecular form.

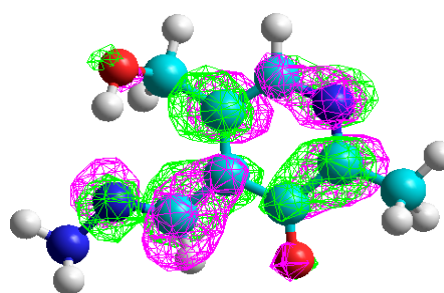


**Fig. 11b: Lowest Unoccupied Molecular Orbitals (LUMO) in Ionized Form**  
Eigen Value -3.60 eV

compounds with biological activity. QSAR properties [21, 22] like surface area, volume, hydration energy, logP, refractivity, polarisability and mass were computed (**Table-4**).

Log P is critical parameter as it gives information about how molecules cross the cell membrane and is important in receptor interactions in biological systems. The low Log P value in PCHHMMH indicates its hydrophilic nature.

**Table 4: QSAR properties of PCHHMMH**

QSAR properties	
Surface area(Approx.)	293.27 Å <sup>2</sup>
Surface area(Grid)	393.59 Å <sup>2</sup>
Volume	572.4 Å <sup>3</sup>
Hydration energy	-18.20 kcal/mol
Log P	0.42
Refractivity	45.4 Å <sup>3</sup>
Polarisability	18.9 Å <sup>3</sup>
Mass	181.19 amu

#### Spectro-analytical studies of Cu (II) complex of PCHHMMH

As the title compound has potential donor sites, we planned to synthesize its Cu (II) complex and characterize by Mass, IR, UV-Vis, TGA, SEM and ESR studies.

#### Mass spectrum

The mass spectrum of Cu (II) PCHHMMH was presented (**Fig.12**).

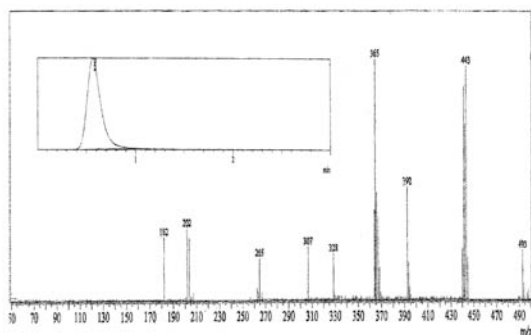


**Fig. 12: LC-MS Chromatogram and Mass Spectrum of Cu (II) PCHHMMH**

From the results it was observed that the molecular ion peak is recorded at  $m/z = 365$  in the mass spectrum of Cu (II) PCHHMMH complex (**Fig.12**). This peak corresponds to 1:1 composition of metal complex. (Cu (II): PCHHMMH) and also infers the presence of Chloro and aquo groups in coordination sphere.

#### IR Spectrum of the Cu (II) PCHHMMH complex

IR spectrum was recorded for the Cu (II) PCHHMMH complex and compared with the spectrum of candidate compound (PCHHMMH)

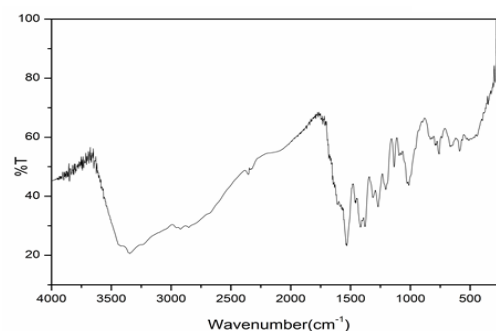


**Fig. 13: IR spectrum of Cu(II) complex of PCHHMMH**

The IR results of the Cu (II) complex (**Fig.13**) displayed trough in the range about 3500-2900  $\text{cm}^{-1}$  indicating presence of coordinated water. The N-H, aromatic and aliphatic C-H vibrations expected in the same region are masked by vibrational modes from water molecules in the complex. The band due to C=N shifted to lower wave number 1531  $\text{cm}^{-1}$  suggests imine nitrogen as one of the donor site for complex formation. The new bands due to M-N M-O bonds and M-Cl in the complex were observed in the far IR (600-400  $\text{cm}^{-1}$ ) region.

#### TGA and DTA studies of Cu (II) PCHHMMH complex

From the TGA of Cu (II) PCHHMMH complex (**Fig.14**), it is observed that the total loss of 75.85 % occurred in three steps. A minimum weight loss in the range of 194-294°C and maximum weight loss in the range of 300-635°C are attributed to loss of coordinated water molecule and ligand through decomposition. The mass of the final residue correspond to the stable copper oxide.

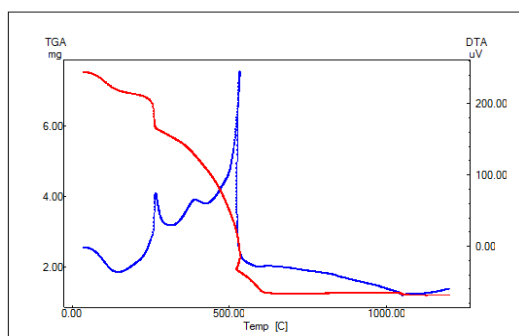


**Fig. 14:** TGA and DTA curves of Cu (II) PCHHMMH complex

The percentage of the metal oxide residue at 1000°C approximately corresponds to metal content in 1:1 composition of the complex. The DTA curve exhibited three exothermic peaks centered at 316°C, 426°C and 500°C which are due to phase changes accompanied by the loss of water followed by the decomposition of coordinated moiety consisting of three nitrogen atoms.

#### SEM and EDX studies of Cu (II) complex of PCHHMMH

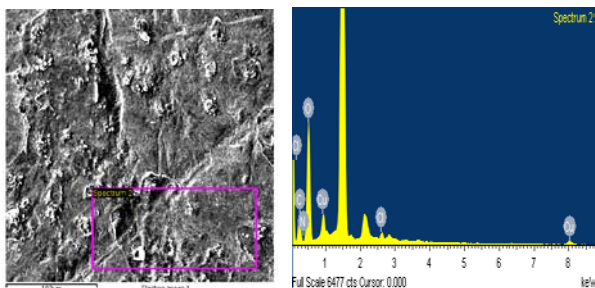


**Fig. 15:** SEM Image and EDX spectrum of Cu (II) complex of PCHHMMH

The Scanning electron microscopy (SEM) image indicated the particle size in the range of 100 $\mu\text{m}$  and EDX results (**Fig.15**) assign the presence of chorine and composition of other elements in the Cu(II)PCHHMMH complex.

#### UV-VIS spectra of PCHHMMH and its Cu (II) complex of PCHHMMH

The electronic spectrum (**Fig.16a**) of title compound and its Cu (II) complex were recorded in dil. acetic acid (1:1) medium at room temperature.

#### PCHHMMH complex

The results indicate the absorption maxima at wavelengths  $\lambda$  of 349nm, 299nm and 227 nm. These peaks may be assigned to  $\pi \rightarrow \pi^*$  (C=C),  $n \rightarrow \pi^*$  (C=N) and  $n \rightarrow \pi^*$  (N=N) transitions respectively. The

bands observed in the visible region of Cu (II) complex spectrum (**Fig.16b**) are attributable to d-d transitions.

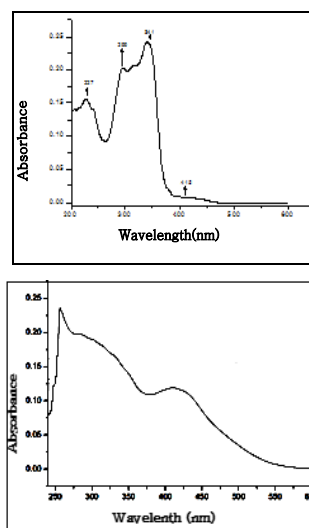


**Fig. 16a:** Uv-Vis spectrum of PCHHMMH **Fig. 16b:** Uv-Vis spectrum of Cu (II)

#### ESR spectrum of Cu (II) complex of PCHHMMH

The ESR spectrum (**Fig.17**) of Cu (II) PCHHMMH complex was recorded in powder state at room temperature.

The results obtained indicated a single peak at 3309G with 'g' value 2.10256. In majority of Cu (II) complexes the 'g' value is anisotropic because of tetragonal distortion. In the present investigation, experimental g value confirms isotropy of Cu (II) PCHHMMH complex inferring less significance of tetragonal distortion. The hyperfine interactions are not observed as the spectrum is recorded in powder state with less energetic X-band radiation.

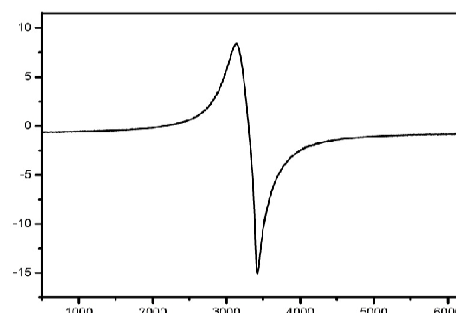


**Fig. 17:** ESR spectrum of Cu (II) PCHHMMH complex.

The magnetic moment ( $\mu$ ) value of Cu (II) PCHHMMH complex calculated from magnetic susceptibility values measured by Faraday method [23, 24] is 1.41 BM.

#### Biological Activity Studies

Antibacterial and cytotoxic activities of the title compound and its complex were evaluated to understand implication of metal ion coordination with binding sites of the hydrazone under study.

#### Antibacterial Activity

The antibacterial activity of the title compound 4-pyridine carboxaldehyde 3-hydroxy-5-(hydroxy methyl)-2-methyl hydrazone (PCHHMMH) hydrochloride was studied by applying the disc diffusion method [25] which is one of the most precise and reliable methods for determining the degree of sensitivity of microbes to antibiotics. The actively growing cultures were mixed in soft agar (1% Nutrient agar were used for bacteria respectively) and plated to

permit fast and good growth yields for many bacterial species. Extract was loaded onto 6mm sterile filter paper discs separately. The discs were then placed on the pre-seeded agar medium and incubated for 24 hrs at 37°C and observed for zone of growth inhibition. The compounds were tested for antibacterial activity against *Staphylococcus aureus*, *Bacillus cereus* (Gram positive) and *Escherichia coli*, *Klebsiella pneumoniae* and *Pseudomonas aeruginosa* (Gram negative) bacteria. The comparison of biological activity with

different strains of bacteria revealed that the compound under investigation is highly active against both gram positive and negative bacteria. The results are tabulated (Table-5). The studies revealed that PCHHMMH showed moderate activity while its copper complex exhibited more pronounced activity against gram-negative bacteria and gram-positive bacteria. The enhanced activity in metal complex indicates the significant role of metal ions in the coordinated system in biological applications.

**Table 5: Antibacterial activity of PCHHMMH and its Cu (II) complex**

Name of the bacteria	Ligand Activity	Cu (II) complex activity	Ampicillin
<b>Gram positive</b>			
<i>Staphylococcus aureus</i>	5+0.4	10+0.4	32+0.1
<i>Bacillus cereus</i>	7.5+0.5	21+0.5	24+0.2
<b>Gram negative</b>			
<i>Pseudomonas aeruginosa</i>	15+0.8	20+0.6	17+0.1
<i>Escherichia coli</i>	7.5+0.5	30+0.5	17+0.1
<i>Klebsiella pneumoniae</i>	NA	NA	18+0.2
<10mm (slightly active), <20mm (moderately active), >20mm (highly active)			

Note: Zone of inhibition is measured in mm, Ampicillin used as a control., NA= Not Active

#### Cytotoxic studies of Cu (II) PCHHMMH complex

The human prostate cancer (DU145), human lung cancer (A549), human breast adenocarcinoma (MCF-7) and human cervical cancer (HeLa) cell lines were obtained from ATCC (Manassas, USA) and maintained in DMEM medium (Sigma), containing 10 % fetal bovine serum, 100 units/mL penicillin and streptomycin. The cytotoxic potential of the Cu(II) complex of 4-pyridine carboxaldehyde-3-hydroxy-5-(hydroxy methyl)-2-methyl hydrazone (PCHHMMH) hydrochloride on these selected tumor cells was measured by Sulforhodamine B (SRB) method. Briefly, the cells are cultured in 96-well plates (5,000 cells/100  $\mu$ L) by incubation for 18-24hrs with constant supply of 5 % CO<sub>2</sub>.

The Cu (II) PCHHMMH complex and doxorubicin as control were prepared in DMSO and added to cell-culture medium at final concentration of 0.1, 1, 10 and 100  $\mu$ M. Plates were incubated further for 48 h. The assay was terminated by the addition of 50  $\mu$ L of cold 10 % trichloro acetic acid (TCA) and incubated for 60 min at

4°C. The plates were washed four times with tap water and air-dried. Sulforhodamine B (SRB) solution (50  $\mu$ L) at 0.057 % (w/v) in 1 % acetic acid was added to each well, and plates were incubated for 30 minutes at room temperature. The excess dye was removed by washing with 1 % acetic acid and the plates were air-dried. The stain bound to cells was solubilized in 10 mM tris base, and the absorbance ( $\lambda_{max}$ ) was measured at 510 nm. From the observed percentage growth for test wells relative to control wells, IC<sub>50</sub> values were calculated.

The cytotoxicity results of the Cu (II) PCHHMMH complex against cancer cell lines were presented in the above table (Table.6) signify the moderate activity towards MCF-7, DU145 and A549 cell lines and inactivity against the HeLa cell line. As the lower IC<sub>50</sub> value corresponds to higher therapeutic activity, the Cu (II) PCHHMMH complex activity order against cancer cell lines is MCF-7 > A549 > DU145. The decreasing order of cytotoxicity indicates that Cu (II) PCHHMMH complex is more active against MCF-7 cell line compare to other cell lines.

**Table 6: Cytotoxicity of Cu (II) PCHHMMH complex on Cancer cell lines**

S. No.	Type of the cancer cell line	Sample	Standard
		Cytotoxicity of the Cu (II) PCHHMMH complex	Doxorubicin IC <sub>50</sub> Values( $\mu$ M) with respect to cancer Cell lines
1	HELA	NA	7.924971
2	MCF-7	44.28	8.8557994
3	DU145	68.72	6.838124
4	A549	45.0396	8.637747

#### CONCLUSION

The study on structural properties of title compound with theoretical and experimental approach indicated corroborated results. The pH-metric and spectrophotometric studies are informative in understanding metal ion binding properties of hydrazone under present study. The spectroanalytical results of copper complex are informative in understanding the structure of complex. Antibacterial studies showed more pronounced activity of copper complex than the title hydrazone in unbound form. Such an inference throws an insight on the activity of metal ions through formation of metal complexes. Further, cytotoxic studies indicated the activity of copper complex against various types of cancer cell lines.

#### CONFLICT OF INTERESTS

Declared None

#### ACKNOWLEDGEMENT

We are thankful to Department of Chemistry, Sarojini Naidu Vanitha Maha Vidyalaya, Hyderabad for providing necessary facilities and Department of Botany for Antimicrobial studies. We are thankful to IICT, Tarnaka, Hyderabad for extending facilities for recording Mass spectra. We are also thankful to the Instrumentation Lab Facilities, Department of Chemistry and CFRD, Osmania University, Hyderabad for recording UV-Vis, IR, <sup>1</sup>H and <sup>13</sup>C NMR spectra. We are thankful to Department of Physics, O.U for recording SEM (EDX) spectra. Our thanks extend to Instrumentation Lab facilities, College of Technology, O.U. for recording TGA and DTA spectra.

#### REFERENCES

- Mayer DE, Rohrer JS, Schoeller DA, Harris DC. Fate of oxygen during ferritin iron incorporation. J Biochemistry 1983;22(4):876-80.

2. Ponka P, Grady RW, Wilczynska A, Schulman HM. The effect of various chelating agents on the mobilization of iron from reticulocytes in the presence and absence of pyridoxal isonicotinoyl hydrazone. *J Biochim Biophys Acta* 1984;802(3):477-89.
3. Theil E, Meister EA. *Advances in Enzymology*, Ed;wiles;New York;1990.p.421-48.
4. Ponka P, Borová J, Neuwirt J, Fuchs O. Mobilization of iron from reticulocytes. Identification of pyridoxal isonicotinoyl hydrazone as a new iron chelating agent. *J FEBS Lett* 1979;97(2):317-21.
5. Ponka P, Borova J, Neuwirt J, Fuchs O. Necas, e. *Biochim, Biophys, Acta* 586,278. *J Biochemistry* 1983.
6. John T, Francis L, Mario E. chubb and P. Ponka *et al.* *J Chemeng Data.*1988;33
7. Irving H, Rossetti HS. M and *J Chem Soc* 3397 1953.
8. Irving H, Rossotti HS. M and *J Chem Soc* 2904 1954.
9. Irving H, Rossotti HS. M and *J Acta Chem Scand* 72.10(1956).
10. Hoi NP. *J Chem Soc* 1358. *Biochemistry* 1953.
11. Craig JC, Edger J. *Nature (London).* *J Biochemistry* 34(1955).
12. Mohan M, Kumar A, Kumar M. *J Inorg Chim Acta Biochemistry.*65(1987).
13. Eshwari P, Int J, Vol S. K.Saroja and Ch. J Sarala Devi of *Pharm and pharm* 1. 2014;6:167-73.
14. Padmaja A, Rajasekhar C, Muralikrishna A, Padmavathi V. Synthesis and antioxidant activity of oxazolyl/ thiazolyl sulfonylmethyl pyrazoles and isoxazoles. *Eur J Med Chem* 2011;46(10):5034-8.
15. Per B. A. Ab-initio and Semi empirical Calculations of Geometry. *J Biochemistry*
16. A. DN. Electronic Spectra of Ru complexes and Modeling. *J Inorg Chem* 1997;36:2544-53.
17. Gilpin NMR, Predicting ID, R. NM. R. K. *Analytical Chemistry;(Iss A541)* 67. *J Biochemistry* 1995;17.
18. Hyperchem V. O. 4.5 for Windows. *J of Chemical Information and Computer Sci Biochemistry* 1996;36 (3):612-4.
19. W R. Winchester and MPDoyle Hyperchem. *J of the American Chemical Society* 1992;114(23)9243.
20. W. Witanowski et al, Solvent effects on the nitrogen NMR shieldings in oxadiazole systems, *J. Magnetic Resonance Biochemistry* 1996;120(2):148-54.
21. Hypercube S, Florida USA. Hyper Chem Florida Science and Technology Park,1115 NW, 4th Street, Gainesville,, 12. *J Biochemistry* 2006;326001.
22. Hansch C, Hoekman D, Leo A, Zhang L, Li P. The expanding role of quantitative structure-activity relationships (QSAR) in toxicology. *J Toxicol Lett* 1995;79(1-3):45-53.
23. Srivastava N, Nath R, Shanker K, Bhargava KP, Kishor K. New indolic cysticidal agents. *J Die Pharmazie* 1977;32(12):756-7.
24. Nicholas D, C. J, Jr HJ, Emeleus R. *Comprehensive Inorganic Chemistry*, ed (by Nyholm & A.F. Trotman), Discussion pergamon press, N 10891978.
25. Pavithra Vani Karsha and O. Bhagya Lakshmi. *J Natural Product Radiance and Resources* 2010;1(2):213-5.